

Structural measurements and vessel density of spectral-domain optic coherence tomography in early, moderate, and severe primary angle-closure glaucoma

Wei Jiang, Nan Jiang, Gui-Bo Liu, Jing Lin, Cui Li, Gui-Qiu Zhao

Department of Ophthalmology, the Affiliated Hospital of Qingdao University, Qingdao 266000, Shandong Province, China

Co-first authors: Wei Jiang and Nan Jiang

Correspondence to: Gui-Qiu Zhao. Department of Ophthalmology, the Affiliated Hospital of Qingdao University, 16 Jiangsu Road, Qingdao 266000, Shandong Province, China. zhaoguiqiu_good@126.com

Received: 2022-05-17 Accepted: 2023-05-16

Abstract

• **AIM:** To compare the macular ganglion cell-inner plexiform layer (GCIPL) thickness, retinal nerve fiber layer (RNFL) thickness, optic nerve head (ONH) parameters, and retinal vessel density (VD) measured by spectral-domain optical coherence tomography (SD-OCT) and analyze the correlations between them in the early, moderate, severe primary angle-closure glaucoma (PACG) and normal eyes.

• **METHODS:** Totally 70 PACG eyes and 20 normal eyes were recruited for this retrospective analysis. PACG eyes were further separated into early, moderate, or severe PACG eyes using the Enhanced Glaucoma Staging System (GSS2). The GCIPL thickness, RNFL thickness, ONH parameters, and retinal VD were measured by SD-OCT, differences among the groups and correlations within the same group were calculated.

• **RESULTS:** The inferior and superotemporal sectors of the GCIPL thickness, rim area of ONH, average and inferior sector of the retinal VD were significantly reduced (all $P < 0.05$) in the early PACG eyes compared to the normal and the optic disc area, cup to disc ratio (C/D), and cup volume were significantly higher (all $P < 0.05$); but the RNFL was not significant changes in early and moderate PACG. In severe group, the GCIPL and RNFL thickness were obvious thinning with retinal VD were decreasing as well as C/D and cup volume increasing than other three groups (all $P < 0.01$). In the early PACG subgroup, there were significant positive correlations between retinal VD and GCIPL thickness (except superonasal and inferonasal sectors, $r = 0.573$ to 0.641 ,

all $P < 0.05$), superior sectors of RNFL thickness ($r = 0.055$, $P = 0.049$). More obvious significant positive correlations were existed in moderate PACG eyes between retinal VD and superior sectors of RNFL thickness ($r = 0.650$, $P = 0.022$), and temporal sectors of RNFL thickness ($r = 0.740$, $P = 0.006$). In the severe PACG eyes, neither GCIPL nor RNFL thickness was associated with retinal VD.

• **CONCLUSION:** The ONH damage and retinal VD loss appears earlier than RNFL thickness loss in PACG eyes. As the PACG disease progressed from the early to the moderate stage, the correlations between the retinal VD and RNFL thickness increases.

• **KEYWORDS:** optic coherence tomography; primary angle-closure glaucoma; ganglion cell-inner plexiform layer; retinal nerve fiber layer; optic nerve head; retinal vessel density

DOI:10.18240/ijo.2023.07.15

Citation: Jiang W, Jiang N, Liu GB, Lin J, Li C, Zhao GQ. Structural measurements and vessel density of spectral-domain optic coherence tomography in early, moderate, and severe primary angle-closure glaucoma. *Int J Ophthalmol* 2023;16(7):1100-1109

INTRODUCTION

Glaucoma is a neurodegenerative disorder as well as the second major contributor of irreversible blindness across the globe^[1]. It is accompanied by an increase in intraocular pressure (IOP), characteristic expansion of the cup to disc ratio (C/D)^[2] of the optic nerve head (ONH), and corresponding damage of visual field (VF)^[3]. In 2040, primary angle-closure glaucoma (PACG) is projected to affect 32.04 million individuals across the globe. In Asia, the incidence of PACG^[4] is much higher than other forms of glaucoma^[4], such as primary open angle glaucoma (POAG). In addition, many investigations have shown that PACG is 3 times more likely than POAG to suffer severe, bilateral visual impairment^[5-6]. PACG is usually related to females, shallow anterior chambers, thickened lenses, hyperopia, and short axial ranges^[7-8]. PACG is characterized by glaucomatous visual damage. In the early phases of PACG, like the preclinical or intermittent

stages, or primary angle closure, optic nerve damage is undetectable^[9]. It is well known that typical structural damage in PACG appears earlier than VF damage. Therefore, apoptosis of ganglion cells, reduction of retinal nerve fiber layer (RNFL) thickness, and the apparent change of ONH parameters are more suitable for the early diagnosis of PACG, while VF and other parameters are more suitable for the staging and monitoring of PACG. As the disease advances, the pattern standard deviation of PACG eyes tends to decrease gradually, accompanied by a more diffuse field loss as the disease progresses^[10].

Optical coherence tomography (OCT) is widely used in glaucoma because of its ability to visualize retinal substructures, including the macula, ONH, and peripapillary area. Compared to the time domain optical coherence tomography, spectral domain optical coherence tomography (SD-OCT) technology quantifies various structural lesions of the optic nerve in glaucoma with unprecedented resolution. In addition to the traditional mechanical theory, vascular theory has become increasingly important in the pathogenesis of glaucoma, and the apoptosis of ganglion cells may be related to local blood flow changes. By using of the motion of red blood cells as an intrinsic contrast agent, optical coherence tomography angiography (OCTA) can quickly and noninvasively create reproducible images of microvascular networks. And due to the widespread use of OCTA, many studies found that retinal vessel density (VD) changes play an important part in the progress of glaucoma^[11-14]. In addition, OCT is more sensitive than VF testing in detecting the progression of PACG.

Numerous studies regarding the use of SD-OCT and OCTA in PACG has emerged in recent years. In the PACG eyes, the average thickness of macular ganglion cell-inner plexiform layer (GCIPL) and RNFL was generally thinner, especially in the inferior, superior, inferotemporal, and superotemporal regions, the ONH parameters changed, and VD decreased. And the microvascular compromise is in fact secondary to structural changes. No studies have explored the differences in structural parameters and VD loss and the correlation between them in various stages of PACG. By comparing the changes of SD-OCT and OCTA parameters in different stages of PACG eyes, we can further understand and explore the characteristics and mechanism of fundus damage in PACG eyes, and subsequently guide the monitoring of disease progression in patients with PACG in clinical diagnosis and treatment, to achieve better clinical therapeutic effect. Therefore, the goal of this current investigation is to explore the macular GCIPL thickness, RNFL thickness, ONH parameters, and retinal VD loss, then compare the characteristics of them among different groups and study the correlations between retinal VD and GCIPL thickness or

RNFL thickness within the same group of PACG eyes and normal eyes by SD-OCT.

SUBJECTS AND METHODS

Ethical Approval The Affiliated Hospital of Qingdao University Ethical Committee and Review Board approved the study procedure and the approval number is QYFY WZLL 27372, which followed the principles of the Declaration of Helsinki. All of the participants received detailed information about the operational choices, as well as signed informed consent documents.

Subjects From July 2019 until December 2020, 70 PACG eyes and 20 normal eyes were recruited in this retrospective cross-sectional research. All subjects underwent comprehensive eye testing such as the visual acuity measurement using the eye chart, IOP measurement by Goldman applanation tonometer, refractive error by the noncycloplegic refraction, corneal pachymetry and anterior segment measurement by Pentacam and IOL Master, slit-lamp examination, gonioscopy, the fundus examination, Octopus VF analysis and SD-OCT.

The criteria of inclusion for PACG patients had to be over the age of 18 and best-corrected visual acuity in the eyes examined at least 20/40, with a refractive error between -6.00 and +3.00 D, and the closed-angle confirmed by gonioscopy. Patients were disqualified if they had previous ocular surgery or had some other ocular disorder. Glaucomatous optic disc neuropathy was defined as C/D difference ≥ 0.2 , large cupping (vertical C/D > 0.6), minimal neural width < 0.1 , or disc hemorrhage.

PACG patients were further divided into early, moderate, and severe PACG by the Enhanced Glaucoma Staging System (GSS2)^[15]. The GSS2 was shown to correctly classify both damage severity and perimetric defect type, using either the corrected or uncorrected VF parameters such as the mean deviation, corrected loss variance or loss variance, corrected pattern standard deviation or pattern standard deviation. In this classification chart, we defined the eyes in stage 0, border and S1 as early PACG group ($n=20$), eyes in S2 and S3 cases as moderate PACG group ($n=24$), and eyes in S4 and S5 as severe PACG group ($n=26$). We have defined the early PACG eyes in stage 0 and border as S0, the remaining early PACG eyes belong to S1. The research only included participants who were identified as having glaucomatous optic disc changes by both observers. Additionally, fixation losses of no more than 20 percent and the ratio of false-positive to false-negative of no more than 15 percent were accepted to describe a reliable VF. The normal group also had to be over the age of 18 and best-corrected visual acuity in the eyes examined at least 20/40, with a refractive error between -6.00 and +3.00 D, IOP of ≤ 21 mm Hg, open angle confirmed by gonioscopy and no history of previous ocular surgery or disorder.

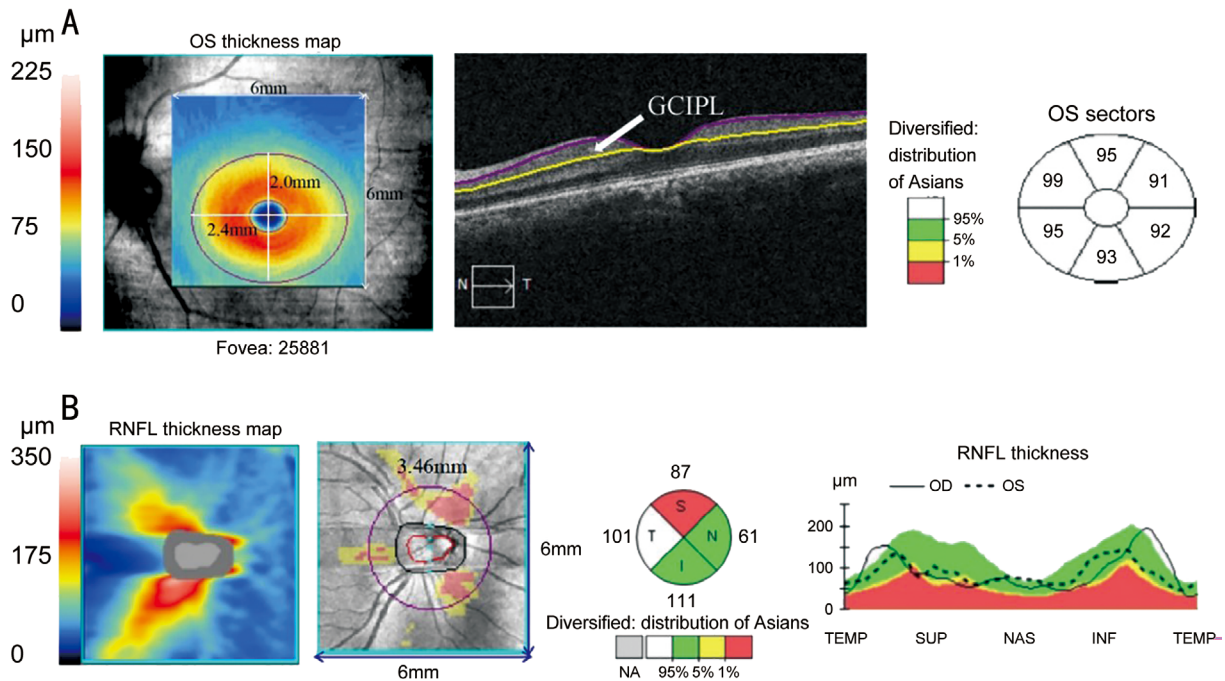


Figure 1 Structural parameters A: Macular ganglion cell-inner plexiform layer (GCIPL) parameters obtained by spectral-domain optic coherence tomography (SD-OCT); B: Retinal nerve fiber layer (RNFL) and optic nerve head (ONH) parameters obtained by SD-OCT.

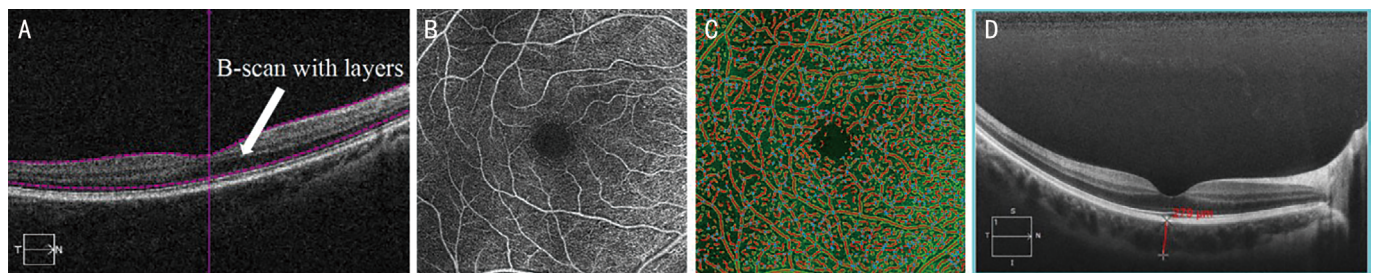


Figure 2 Vessel density and choroidal thickness parameters A, B: Retinal vessel density (VD) obtained by optic coherence tomography angiography (OCTA); C: Retinal VD detected by AngioTool software; D: Choroidal thickness obtained by SD-OCT (HD 1 Line 100x).

SD-OCT Measurements Images of macular, peripapillary RNFL, optic disc head, retinal VD, and choroid were all acquired by the cirrus SD-OCT (Carl Zeiss Meditec, Inc., Germany). The SD-OCT built-in software ganglion cell analysis pattern was applied to calculate macular GCIPL thickness in a $6 \times 6 \times 2 \text{ mm}^3$ cube based on the fovea. In an elliptical annulus, the GCIPL sectoral thicknesses were measured (the diameters of each sector are 1, 4, 1.2, and 4.8 mm)^[16-18].

A $6 \times 6 \times 2 \text{ mm}^3$ data cube with 200×200 axial scanning was used to create the optic disc cube image. The facilities created a round B-scan with a diameter of 3.46 mm from these results, accompanied by the pattern intelligently located and positioned the central optic disc. Then the system determined the thickness of the RNFL at each position around the circle and showed the results^[19].

The average, minimum, and sectoral (superonasal, superior, superotemporal, inferotemporal, inferior, inferonasal quadrants) variables were used to evaluate the macular GCIPL thickness (Figure 1A). The average and sectoral (superior,

inferior, temporal, and nasal quadrants) parameters were involved in the peripapillary RNFL thickness measurements (Figure 1B). Individual parameters in the ONH measurements included rim area, disc area, average C/D, vertical C/D, and cup volume (Figure 1B). The high-quality pictures with a signal intensity of at least 3 were used.

The retinal VD was measured using the cirrus OCTA. The Scan generates a $6 \times 6 \text{ mm}^2$ square cube and is similar to the macular cube 200×200 scans but it employs an intensity-based frequency filtering technique to produce images with detailed vasculature (Figure 2A-2C). HD 1 Line 100x was performed to acquire the retinal and choroid image in the macular region with central fixation. This scan produces a single high-definition scan with 100 B-scans, each made of 1024 A-scans, with a line length of 9 mm at a depth of 2.0 mm. After obtaining the scanned image, the choroidal thickness was measured manually (Figure 2D).

Pentacam Measurements With a revolving Scheimpflug camera, the Pentacam imaged the anterior segment of the eye, performing up to 50 scanning, each with 500 images, for a

Table 1 Demographic and clinical characteristics of study subjects

Parameters	Normal: group 1 (n=20)	Early: group 2 (n=20)	Moderate: group 3 (n=24)	Severe: group 4 (n=26)	mean±SD P
Age, y	67.45±2.48	68.78±4.20	66.75±6.16	72.80±6.89	0.001
Sex, female/male	9/11	14/6	17/7	16/10	0.304
Diabetes mellitus	2/18	2/18	3/21	4/22	0.911
Systemic hypertension	3/17	4/16	7/17	8/18	0.577
Smoking ratio	1/19	1/19	2/22	3/23	0.909
IOP, mm Hg	17.21±0.98	25.33±1.03	27.12±1.55	27.25±0.97	<0.001
Axial length, mm	24.57±1.06	23.02±0.40	22.41±0.69	22.88±0.33	<0.001
CCT, μm	535.60±30.96	529.67±27.57	544.80±28.70	541.60±32.05	0.256
Choroidal thickness, μm	257.32±11.43	251.70±10.43	283.60±14.71	277.21±14.60	0.225
Lens thickness, mm	3.59±0.05	5.05±0.26	5.22±0.04	5.00±0.06	<0.001
WTW, mm	11.94±0.09	11.40±0.16	11.39±0.08	11.31±0.09	<0.001
ACA, degrees	42.85±0.31	24.60±1.69	20.22±1.65	24.98±1.65	<0.001
CACD, mm	2.95±0.16	1.81±0.08	1.62±0.17	1.92±0.11	<0.001
ACV, mm ³	162.09±16.03	74.25±4.28	61.28±3.38	61.82±4.10	<0.001

Comparison of normal, early, moderate, and severe primary angle-closure glaucoma groups using one-way ANOVA, Welch's ANOVA, Fisher's exact test or Pearson Chi-square. SD: Standard deviation; IOP: Intraocular pressure; CCT: Central corneal thickness; WTW: White-to-white corneal diameter; ACA: Anterior chamber angle; CACD: Central anterior chamber depth; ACV: Anterior chamber volume.

total of 25 000 true data points (measurement and elevation points). The system calculated the central corneal thickness, the anterior chamber angle (ACA), the anterior chamber volume (ACV), height, and diameter at any location in the anterior chamber. The distance between the endothelium at the corneal apex and the anterior lens capsule was assessed with the Pentacam to determine central anterior chamber depth (CACD). ACV was calculated automatically by Pentacam after the rotating scan^[20-21].

IOL Master Measurements The IOL Master 700 (Carl Zeiss Meditec AG, Jena, Germany) used an SS-OCT pattern to obtain anterior segment data, like lens thickness (LT), horizontal white-to-white (WTW) corneal diameter, pupil size, and axial length (AL).

Statistical Analysis Statistical analyses about the parameters were conducted with SPSS version 26.0 (SPSS Inc., Chicago, Illinois, USA). AngioTool software was used for quantitative analysis of OCTA. All of the demographic and clinical characteristics, the thickness of the peripapillary RNFL, macular GCIPL, ONH parameters, and VD data were analyzed among the normal eyes, early PACG, moderate PACG, and severe PACG eyes using one-way ANOVA and Welch's ANOVA. Pairwise comparisons between any two groups were used for each of the individual parameters. The relationships between retinal VD and GCIPL or RNFL thickness were assessed by using the Pearson correlation coefficient. $r < 0.3$ indicated a minor correlation; $0.3 \leq r < 0.6$, a medium correlation; $r \geq 0.6$ indicated a powerful correlation. The statistical difference was considered significant if $P < 0.05$.

RESULTS

Subjects Totally 90 eyes (20 normal eyes, 20 early PACG

eyes, 24 moderate PACG eyes, and 26 severe PACG eyes) were included. Table 1 showed the baseline data among the four groups.

Table 2 revealed the detailed comparisons of the macular GCIPL thickness, peripapillary RNFL thickness, ONH parameters, and retinal VD among the 4 groups.

GCIPL Thickness All regions of the GCIPL thickness in the early PACG subgroup were thinner than normal group, but only in the inferior and superotemporal regions differed significantly between the two ($P=0.019$, $P=0.005$). Almost every quadrant of the GCIPL thickness in the early PACG subgroup was thicker than moderate PACG group, but we found no statistical differences between them (all $P > 0.05$). In all regions of the GCIPL thickness, the severe PACG eyes demonstrated significant thinner than the early or moderate PACG group (all $P < 0.001$; Table 2).

RNFL Thickness Between the normal and early PACG group, all regions of RNFL thickness noted no statistical differences (all $P > 0.05$). In each quadrant of RNFL thickness, no statistical differences were revealed between the early and moderate PACG eyes (all $P > 0.05$). The RNFL thickness of moderate PACG group was considerably greater than that of severe PACG in all regions except for the temporal location ($P < 0.001$, $P=0.041$, 0.043 respectively). In addition, each sector of RNFL in the early PACG was considerably thicker than that in the severe PACG eyes ($P < 0.001$, $P=0.004$, 0.007 , 0.002 respectively; Table 2).

Optic Nerve Head Parameters The rim area of the normal group highlighted greater values when compared to the early PACG group ($P < 0.001$). The optic disc area, average C/D, vertical C/D, and cup volume of the early PACG eyes were all

Table 2 Macular GCIPL, RNFL thickness, ONH, and retinal VD parameters obtained by SD-OCT

Parameters	Normal: group 1 (n=20)	Early: group 2 (n=20)	Moderate: group 3 (n=24)	Severe: group 4 (n=26)	P^1	P^2	P^3	P^4	mean±SD
GCIPL, μm									
Average	82.45±6.77	78.79±6.49	78.26±4.48	52.08±18.13	0.199	0.974	<0.001	<0.001	
Minimum	76.60±6.08	76.21±6.64	73.63±5.60	40.67±19.91	0.997	0.594	<0.001	<0.001	
Superior	82.70±7.22	78.11±7.16	78.74±9.53	55.00±19.47	0.152	0.978	<0.001	<0.001	
Inferior	83.70±6.69	77.42±6.87	78.11±6.66	50.54±16.99	0.019	0.974	<0.001	<0.001	
Superonasal	83.25±8.09	79.84±7.06	79.47±9.36	55.13±22.60	0.505	1.000	<0.001	<0.001	
Inferonasal	82.35±7.26	79.16±6.51	82.11±5.45	52.00±20.80	0.479	0.455	<0.001	<0.001	
Superotemporal	83.60±4.87	77.32±6.51	76.95±5.33	50.00±18.82	0.005	0.994	<0.001	<0.001	
Inferotemporal	78.90±5.80	76.74±8.04	75.16±9.26	49.67±16.30	0.629	0.982	<0.001	<0.001	
RNFL, μm									
Average	93.00±6.78	93.00±8.41	93.17±24.12	57.11±5.14	1.000	0.974	<0.001	<0.001	
Superior	106.35±14.83	113.70±11.69	111.74±37.83	63.89±5.96	0.318	0.995	0.041	0.004	
Inferior	124.40±22.23	114.40±19.85	121.35±40.45	59.21±8.37	0.558	0.928	<0.001	<0.001	
Nasal	70.40±4.67	73.50±12.29	73.09±17.29	61.84±9.35	0.720	1.000	0.043	0.007	
Temporal	82.40±14.99	72.25±9.52	65.00±13.13	45.95±10.14	0.215	0.477	0.087	0.002	
ONH									
Rim area, mm^2	1.55±0.18	1.29±0.13	1.36±0.26	0.72±0.12	<0.001	0.938	<0.001	<0.001	
Optic disc area, mm^2	1.71±0.12	2.00±0.45	1.99±0.39	2.11±0.45	0.042	0.931	0.739	0.401	
Average C/D	0.45±0.08	0.60±0.11	0.52±0.14	0.80±0.04	0.001	0.849	<0.001	<0.001	
Vertical C/D	0.41±0.08	0.55±0.11	0.48±0.17	0.80±0.06	0.001	0.842	<0.001	<0.001	
Cup volume, mm^3	0.05±0.04	0.17±0.10	0.11±0.08	0.49±0.15	<0.001	0.168	<0.001	0.001	
Retinal VD, %									
Average	38.40±1.61	34.91±3.76	34.86±2.24	29.91±3.71	0.030	1.000	0.003	0.011	
Superior	37.59±4.22	37.39±3.14	37.59±2.87	30.77±3.70	0.830	0.617	0.001	0.001	
Inferior	35.69±3.67	31.65±3.43	31.52±2.61	27.77±3.71	0.016	1.000	0.001	0.001	
Nasal	38.04±3.68	36.89±3.32	36.23±3.26	28.26±2.01	0.798	0.943	0.003	0.001	
Temporal	37.62±2.03	34.84±3.81	35.86±2.54	28.89±4.52	0.114	0.835	0.001	0.004	

GCIPL: Ganglion cell-inner plexiform layer; RNFL: Retinal nerve fiber layer; ONH: Optic nerve head; C/D: Cup to disc ratio; VD: Vessel density; SD: Standard deviation. Value for comparison of normal, early, moderate, and severe primary angle-closure glaucoma groups using one-way ANOVA and Welch' ANOVA. P^1 : Group 1 vs Group 2; P^2 : Group 2 vs Group 3; P^3 : Group 3 vs Group 4; P^4 : Group 2 vs Group 4.

significantly greater than the normal group ($P<0.001$, $P=0.042$, 0.001 , 0.001 , <0.001 respectively). All variables seemed not to differ statistically between the early and moderate PACG groups. The rim area of the moderate PACG highlighted greater values than the severe PACG ($P<0.001$). The average C/D, vertical C/D, and cup volume of the severe PACG all documented greater values than the moderate eyes (all $P<0.001$). The early PACG eyes had a greater rim area than the severe PACG eyes ($P<0.001$). The average C/D, vertical C/D, and cup volume of the early PACG eyes were all smaller than the severe PACG eyes ($P<0.001$, <0.001 , 0.001 respectively). The optic disc area of the early PACG eyes was smaller than the severe PACG subgroup, while with no statistical difference ($P=0.401$; Table 2).

Retinal Vessel Density The average and inferior sector of retinal VD in the normal group highlighted significantly greater than the early PACG ($P=0.030$, 0.016 respectively; Table 2). The retinal VD of the severe PACG noted significantly smaller

values than the early and the moderate PACG (Table 2).

Correlations Between Retinal VD and GCIPL or RNFL Thickness In the early PACG group, significant correlations were detected between retinal VD and the average, minimum, superior, inferior, superotemporal, and inferotemporal locations of GCIPL thickness (Table 3). A significant association of retinal VD with superior sectors of RNFL thickness was detected in the early PACG eyes ($r=0.055$, $P=0.049$). In addition, significant positive correlations were found in moderate PACG eyes between retinal VD and superior sectors of RNFL thickness ($r=0.650$, $P=0.022$), and temporal sectors of RNFL thickness ($r=0.740$, $P=0.006$). There was no significant correlation between retinal VD and GCIPL or RNFL thickness in the severe PACG group.

DISCUSSION

Glaucoma is a kind of optic neurodegenerative disease marked by chronic gradual damage of retinal ganglion cells^[22], as well as a typical expansion of the C/D of the ONH, defect of

Table 3 Correlations between retinal vessel density with macular GCIPL and RNFL thickness

Parameters	Retinal vessel density							
	Normal: group 1		Early: group 2		Moderate: group 3		Severe: group 4	
	<i>r</i>	<i>P</i>	<i>r</i>	<i>P</i>	<i>r</i>	<i>P</i>	<i>r</i>	<i>P</i>
GCIPL thickness								
Average	-0.211	0.371	0.591	0.033	0.351	0.320	-0.149	0.644
Minimum	0.102	0.670	0.583	0.047	0.288	0.419	0.104	0.748
Superior	-0.302	0.195	0.641	0.018	0.297	0.404	0.098	0.762
Inferior	-0.216	0.359	0.640	0.018	0.487	0.153	-0.276	0.385
Superonasal	-0.026	0.914	0.521	0.082	0.381	0.278	-0.235	0.462
Inferonasal	-0.253	0.282	0.531	0.076	0.622	0.055	-0.315	0.318
Superotemporal	0.111	0.641	0.573	0.041	0.345	0.328	0.032	0.922
Inferotemporal	-0.121	0.611	0.594	0.032	0.474	0.166	-0.080	0.806
RNFL thickness								
Average	-0.410	0.072	0.366	0.219	0.553	0.062	-0.448	0.167
Superior	-0.301	0.097	0.555	0.049	0.650	0.022	0.402	0.174
Inferior	-0.202	0.393	0.304	0.313	0.440	0.152	0.323	0.282
Nasal	0.275	0.241	-0.190	0.533	0.155	0.631	0.181	0.554
Temporal	-0.068	0.777	0.264	0.384	0.740	0.006	0.336	0.286
ONH parameters								
Rim area	-0.098	0.689	0.369	0.214	0.154	0.633	0.084	0.795
Optic disc area	0.196	0.421	0.352	0.238	0.325	0.330	0.302	0.315
Average C/D	-0.033	0.892	0.103	0.739	0.141	0.662	-0.106	0.744
Vertical C/D	0.224	0.342	0.046	0.882	-0.060	0.853	-0.086	0.789
Cup volume	-0.208	0.380	0.242	0.425	0.226	0.504	-0.055	0.858

The relationships between retinal vessel density and GCIPL or RNFL thickness were evaluated by the Pearson correlation analysis. GCIPL: Ganglion cell-inner plexiform layer; RNFL: Retinal nerve fiber layer; ONH: Optic nerve head; C/D: Cup to disc ratio.

RNFL^[23], and corresponding VF damage. It is the major risk factor contributing to irreversible forms of blindness in the world today. According to a study, the incidence of PACG is much higher in Asia than in other regions^[5,24]. Diagnosis of PACG with different stages is important, though, in clinical practice, precise diagnosis is difficult without comprehensive examination and a longer time. Considering the high prevalence and high underdiagnosis rate of PACG, it is of vital importance to investigate the variation rules of numerical parameters that could help with earlier diagnosis and determine the valuable diagnostic tools, such as the structural parameters acquired by OCT. The ability to detect glaucoma of macular GCIPL thickness, peripapillary RNFL thickness, ONH parameters, and retinal VD by using SD-OCT measurements has been shown in numerous studies^[25-26]. Most Cirrus SD-OCT studies suggest that the inferior, superior, inferotemporal, and superotemporal regions were the most vulnerable areas of glaucoma^[27].

The mean age, IOP, AL, LT, WTW, ACA, CACD, and ACV showed significant differences among the 4 groups. As we all know, short axial length, increased LT, small cornea, and shallow anterior chamber are the risk factors for PACG^[28-29]. With

increasing age, the thickness of the lens gradually increases, resulting in a more crowded anterior chamber structure. This may account for the age difference between the PACG groups and the normal group.

The inferior and superotemporal regions of GCIPL thickness had considerable differences between the normal and early PACG groups. Studies have shown that the thickness of GCIPL on the temporal quadrants is more susceptible than the nasal quadrants with the progression of glaucoma^[30-31]. Most studies have suggested that the temporal, especially inferotemporal areas of macula are the most vulnerable sections^[32]. The studies discovered that the glaucomatous macular damage had a particular occurrence in the inferior area by using OCT^[33], which we call the macular vulnerability zone. Likewise, most areas of the inferior sector of the macula project to the inferior area of the optic disc, which leads to the fact that this quadrant is more prone to glaucomatous damage^[34]. Because PACG progression damage occurred initially locally and there are regional variations in vulnerability, the impact on the average GCIPL thickness was small. Averaging the thickness values obtained from the sector parameters may mask the regional variation of GCIPL. And the macular GCIPL

topography is less variable among normal individuals than other diagnostically important structures, such as the ONH and RNFL, which all result in a superior diagnostic accuracy of macular GCIPL parameters in the early stage of glaucoma. Our study found no significant differences in all regions of the GCIPL thickness between early and moderate PACG subgroup. Between the early and severe PACG eyes, all regions of GCIPL thickness showed significant differences. The same was true for comparison between the moderate PACG eyes and severe PACG eyes. This indicated that GCIPL thickness loss was more localized in the early PACG group and more diffuse in the moderate to severe PACG group.

Compared with GCIPL thickness, the diagnostic power of the RNFL parameters in PACG may be limited because it is only divided into four sectors in SD-OCT, whereas GCIPL is divided into six sectors. There was no significant difference between the RNFL thickness of each quadrant in the early stage of PACG and the normal control group, and so was the comparison between the moderate PACG group and the early PACG group. In all regions except the temporal location of RNFL thickness, the moderate PACG eyes were significantly greater than the severe PACG eyes. In all regions of RNFL thickness, the early PACG eyes were significantly greater than the severe PACG eyes. It has been confirmed that in early glaucoma, the detection of RNFL damage occurs after the detection of GCIPL damage in the corresponding region^[35]. This indicates that the RNFL thickness thinning of PACG occurs slightly later than GCIPL, or the early damage is difficult to detect, while in the moderate and severe stages, the RNFL thickness presents diffuse damage. But studies have also confirmed that the RNFL thickness increased immediately after an attack of PACG eyes^[36]. The previous study has shown that the inferotemporal RNFL thickness was the perfect variable to differentiate the PACG from the normal eyes^[37]. The inferior RNFL was involved in the moderate subgroups of both PACG and POAG^[38]. In the early stage of PACG, RNFL thickness did not change significantly. When the PACG disease progresses to advanced stages, RNFL thickness shows a diffuse loss.

ONH parameters highlighted obvious differences between normal and the early PACG subgroups. It is well known that the direct damage site of elevated IOP is the ONH. And many animal studies have proved that the damage of ONH caused by elevated IOP is earlier than that of ganglion cells and RNFL thickness^[39]. This is consistent with the results of ONH parameters changes in early PACG in our study. The rim area of the moderate PACG eyes was greater than the severe PACG eyes which showed a significant difference. The average C/D, vertical C/D, and cup volume of the severe PACG eyes were all greater than the moderate eyes with statistically significant differences. The same was true of comparisons

between early and moderate PACG groups. A large number of studies have confirmed that best ONH parameters for detecting glaucomatous nerve damage are rim area and vertical C/D ratio^[27]. In our study, the average C/D ratio and vertical C/D ratio damaged first in early PACG eyes. Although the ONH parameters showed great variability in the population, they could show strong differences between the early PACG and the normal eyes.

The study using OCTA has demonstrated the decrease of VD is uniform in PACG^[40-41]. We found the average and inferior location of retinal VD in the normal subgroup noted significantly greater values than the early PACG subgroup, which was consistent with the earlier reports^[42]. As unexpected, no statistical difference was demonstrated in all areas of the retinal VD between the early and moderate PACG group. All locations of the retinal VD of the severe PACG eyes were significantly smaller than the early or moderate PACG eyes. Kim *et al*^[43] found evidence that microvascular compromise is in fact secondary to structural changes. This conclusion is consistent with the fact that in our study, only the average and inferior VD changed significantly in the early stage of PACG, while in the moderate and severe stage of PACG, the VD in each quadrant changed significantly.

The previous study has also shown that the loss of retinal vessel densities occurred later than the structural alterations in PACG eyes^[41]. Our study showed that in the early stage of PACG, the RNFL thickness defect might be undetectable, while the ONH defect had been detected, as well as a loss of some areas of ganglion cells and retinal VD. This suggested that RNFL thickness changes appear later than VD loss, reduction of GCIPL thickness (inferior and superotemporal), and ONH parameters in the early diagnosis of PACG. The causal relationship between the reduced blood perfusion and loss of ganglion cells or reduction of RNFL thickness in glaucoma has long been concerned^[44]. Our study found differences in GCIPL thickness, ONH parameters, and VD between early PACG and the normal group. This indicated that GCIPL thickness, ONH parameters, and VD have all changed in early PACG eyes. This causal relationship between the reduced blood perfusion and structural parameters was still worthy of long-term research.

The sensitivity of GCIPL thickness, RNFL thickness, retinal VD, and ONH parameters damage varied in different regions during the progression of the PACG. In addition, there was a severity-dependent association between retinal VD and GCIPL or RNFL thickness, but with no correlation to the ONH parameters.

It has been found that VD was obviously related to RNFL and GCIPL thickness in glaucoma^[45-46]. However, the correlation between retinal VD and structural parameters in different

stages of PACG was not clear. The dysfunction of retinal ganglion cells in PACG is often accompanied by insufficient blood supply, which was verified in our study. In the early PACG eyes, there were significant positive associations between retinal VD and the average GCIPL, between retinal VD and the minimum GCIPL, between retinal VD and the superior, inferior, superotemporal and inferotemporal locations of GCIPL thickness. One study found strong positive correlations between VD and RNFL thickness in the radial peripapillary capillaries layer for all sectors except the superonasal area^[47]. In our study, the correlation between retinal VD and superior sectors of RNFL thickness in the early PACG eyes was moderate positive. There were significant strong associations between retinal VD and the superior sectors of RNFL thickness, between retinal VD and the temporal sectors of RNFL thickness in moderate PACG eyes. That can only mean that in the early stage to moderate stage of PACG, the more severe the PACG was, the lower VD was. This suggested that in the progress of early stage to moderate stage of PACG, the loss of VD was gradually closely related to the reduced thickness of RNFL. And this is because both RNFL thickness and VF decrease rapidly in early to moderate PACG, while in severe PACG, RNFL thickness reaches a “floor” in which residual non-neural tissue limits the utility of detecting changes in neural tissue. Therefore, there is no significant correlation between RNFL thickness and VD in severe PACG. The current research included two limitations. First, it is retrospective in design. More information will be needed from a long-term and repeatable investigation. Second, there are relatively small numbers of subjects. A prospective study with more PACG eyes will be necessary for a successful further investigation.

In conclusion, the ONH damage and retinal VD loss appeared earlier than RNFL thickness loss in PACG eyes. With the development of PACG disease from early to the moderate stage, the correlations between the retinal VD and RNFL thickness increased.

ACKNOWLEDGEMENTS

Authors' contributions: Jiang W carried out the study and drafted the original manuscript. Zhao GQ and Jiang N conceived of the study and participated in its design and coordination. Liu GB conducted the literature search. Lin J revised the manuscript. Li C conducted the picture processing. All authors contributed to the article and approved the submitted version.

Foundations: Supported by the Youth National Natural Science Foundation of China (No.81700800; No.81800800); the Natural Science Foundation of Shandong Province (No. ZR2017MH008); Taishan Scholar Project of Shandong Province (No.tsqn201812151).

Conflicts of Interest: Jiang W, None; Jiang N, None; Liu GB, None; Lin J, None; Li C, None; Zhao GQ, None.

REFERENCES

- 1 Stein JD, Khawaja AP, Weizer JS. Glaucoma in adults-screening, diagnosis, and management: a review. *JAMA* 2021;325(2):164-174.
- 2 Zhao R, Chen X, Liu X, Chen Z, Guo F, Li S. Direct cup-to-disc ratio estimation for glaucoma screening via semi-supervised learning. *IEEE J Biomed Health Inform* 2020;24(4):1104-1113.
- 3 Sihota R, Selvan H, Sharma A, Gupta N, Shakrawal J, Angmo DW, Dada T, Upadhyay A. Severity of visual field defects in primary congenital glaucoma and their risk factors. *Graefes Arch Clin Exp Ophthalmol* 2020;258(7):1483-1491.
- 4 Zhang N, Wang J, Chen B, Li Y, Jiang B. Prevalence of primary angle closure glaucoma in the last 20 years: a meta-analysis and systematic review. *Front Med* 2020;7:624179.
- 5 Tham YC, Li X, Wong TY, Quigley HA, Aung T, Cheng CY. Global prevalence of glaucoma and projections of glaucoma burden through 2040:a systematic review and meta-analysis. *Ophthalmology* 2014;121(11):2081-2090.
- 6 Allison K, Patel D, Alabi O. Epidemiology of glaucoma: the past, present, and predictions for the future. *Cureus* 2020;12(11):e11686.
- 7 Sun X, Dai Y, Chen Y, Yu DY, Cringle SJ, Chen J, Kong X, Wang X, Jiang C. Primary angle closure glaucoma: what we know and what we don't know. *Prog Retin Eye Res* 2017;57:26-45.
- 8 Sun J, Li T, Zhao X, Lu B, Chen J, Liu W, Zhou M, Sun X. Prevalence and risk factors of glaucoma among Chinese people from the China health and retirement longitudinal study. *J Glaucoma* 2022;31(10):789-795.
- 9 Douglas GR, Drance SM, Schulzer M. The visual field and nerve head in angle-closure glaucoma. A comparison of the effects of acute and chronic angle closure. *Arch Ophthalmol* 1975;93(6):409-411.
- 10 Gazzard G, Foster PJ, Viswanathan AC, et al. The severity and spatial distribution of visual field defects in primary glaucoma: a comparison of primary open-angle glaucoma and primary angle-closure glaucoma. *Arch Ophthalmol* 2002;120(12):1636-1643.
- 11 Rao HL, Pradhan ZS, Suh MH, Moghimi S, Mansouri K, Weinreb RN. Optical coherence tomography angiography in glaucoma. *J Glaucoma* 2020;29(4):312-321.
- 12 Werner AC, Shen LQ. A review of OCT angiography in glaucoma. *Semin Ophthalmol* 2019;34:279-286.
- 13 Shen R, Wang YM, Cheung CY, Chan PP, Tham CC. Comparison of optical coherence tomography angiography metrics in primary angle-closure glaucoma and normal-tension glaucoma. *Sci Rep* 2021;11(1):23136.
- 14 Hou TY, Kuang TM, Ko YC, et al. Optic disc and macular vessel density measured by optical coherence tomography angiography in open-angle and angle-closure glaucoma. *Sci Rep* 2020;10(1):5608.
- 15 Brusini P, Filacorda S. Enhanced glaucoma staging system (GSS 2) for classifying functional damage in glaucoma. *J Glaucoma* 2006;15(1):40-46.

- 16 Mwanza JC, Oakley JD, Budenz DL, *et al.* Macular ganglion cell–inner plexiform layer: automated detection and thickness reproducibility with spectral domain–optical coherence tomography in glaucoma. *Invest Ophthalmol Vis Sci* 2011;52(11):8323.
- 17 Mwanza JC, Durbin MK, Budenz DL, *et al*; Cirrus OCT Normative Database Study Group. Profile and predictors of normal ganglion cell-inner plexiform layer thickness measured with frequency-domain optical coherence tomography. *Invest Ophthalmol Vis Sci* 2011;52(11):7872-7879.
- 18 Curcio CA, Allen KA. Topography of ganglion cells in human retina. *J Comp Neurol* 1990;300(1):5-25.
- 19 Savini G, Carbonelli M, Barboni P. Spectral-domain optical coherence tomography for the diagnosis and follow-up of glaucoma. *Curr Opin Ophthalmol* 2011;22(2):115-123.
- 20 Reuland MS, Reuland AJ, Nishi Y, Auffarth GU. Corneal radii and anterior chamber depth measurements using the IOLmaster versus the Pentacam. *J Refract Surg* 2007;23(4):368-373.
- 21 Rabsilber TM, Khoramnia R, Auffarth GU. Anterior chamber measurements using Pentacam rotating Scheimpflug camera. *J Cataract Refract Surg* 2006;32(3):456-459.
- 22 Yang X, Zeng Q, Tezel G. Regulation of distinct caspase-8 functions in retinal ganglion cells and astroglia in experimental glaucoma. *Neurobiol Dis* 2021;150:105258.
- 23 Freedman SF, Beck AD, Nizam A, Vanderveen DK, Plager DA, Morrison DG, Drews-Botsch CD, Lambert SR; Infant Aphakia Treatment Study Group. Glaucoma-related adverse events at 10 years in the infant aphakia treatment study: a secondary analysis of a randomized clinical trial. *JAMA Ophthalmol* 2021;139(2):165-173.
- 24 Qu W, Li Y, Song W, Zhou X, Kang Y, Yan L, Sui H, Yuan H. Prevalence and risk factors for angle-closure disease in a rural Northeast China population: a population-based survey in Bin County, Harbin. *Acta Ophthalmol* 2011;89(6):e515-e520.
- 25 Renard JP, F enolland JR, Giraud JM. Glaucoma progression analysis by spectral-domain optical coherence tomography (SD-OCT). *J Fr Ophthalmol* 2019;42(5):499-516.
- 26 Kim NR, Lee ES, Seong GJ, Kang SY, Kim JH, Hong S, Kim CY. Comparing the ganglion cell complex and retinal nerve fibre layer measurements by Fourier domain OCT to detect glaucoma in high myopia. *Br J Ophthalmol* 2011;95(8):1115-1121.
- 27 Chen TC, Hoguet A, Junk AK, Nouri-Mahdavi K, Radhakrishnan S, Takusagawa HL, Chen PP. Spectral-domain OCT: helping the clinician diagnose glaucoma. *Ophthalmology* 2018;125(11):1817-1827.
- 28 Zhang Y, Zhang Q, Thomas R, Li SZ, Wang NL. Development of angle closure and associated risk factors: the Handan eye study. *Acta Ophthalmol* 2022;100(1):e253-e261.
- 29 Wang Y, Cun Q, Li J, Shen W, Yang WY, Tao YJ, Niu ZQ, Zhang Y, Zhong H, Pan CW. Prevalence, ethnic differences and risk factors of primary angle-closure glaucoma in a multiethnic Chinese adult population: the Yunnan Minority Eye Study. *Br J Ophthalmol* 2023;107(5):677-682.
- 30 Hood DC, Raza AS, de Moraes CG, Liebmann JM, Ritch R. Glaucomatous damage of the macula. *Prog Retin Eye Res* 2013;32:1-21.
- 31 Lee WJ, Kim YK, Park KH, Jeoung JW. Trend-based analysis of ganglion cell-inner plexiform layer thickness changes on optical coherence tomography in glaucoma progression. *Ophthalmology* 2017;124(9):1383-1391.
- 32 Kim HJ, Jeoung JW, Yoo BW, Kim HC, Park KH. Patterns of glaucoma progression in retinal nerve fiber and macular ganglion cell-inner plexiform layer in spectral-domain optical coherence tomography. *Jpn J Ophthalmol* 2017;61(4):324-333.
- 33 Kim KE, Park KH. Macular imaging by optical coherence tomography in the diagnosis and management of glaucoma. *Br J Ophthalmol* 2018;102(6):718-724.
- 34 Zhang X, Xiao H, Liu C, *et al.* Comparison of macular structural and vascular changes in neuromyelitis optica spectrum disorder and primary open angle glaucoma: a cross-sectional study. *Br J Ophthalmol* 2021;105(3):354-360.
- 35 Kim YK, Ha A, Na KI, Kim HJ, Jeoung JW, Park KH. Temporal relation between macular ganglion cell-inner plexiform layer loss and peripapillary retinal nerve fiber layer loss in glaucoma. *Ophthalmology* 2017;124(7):1056-1064.
- 36 Rao HL, Babu JG, Addepalli UK, Senthil S, Garudadri CS. Retinal nerve fiber layer and macular inner retina measurements by spectral domain optical coherence tomograph in Indian eyes with early glaucoma. *Eye (Lond)* 2012;26(1):133-139.
- 37 Rao HL, Kadambi SV, Weinreb RN, Puttaiah NK, Pradhan ZS, Rao DAS, Kumar RS, Webers CAB, Shetty R. Diagnostic ability of peripapillary vessel density measurements of optical coherence tomography angiography in primary open-angle and angle-closure glaucoma. *Br J Ophthalmol* 2017;101(8):1066-1070.
- 38 Manassakorn A, Aupapong S. Retinal nerve fiber layer defect patterns in primary angle-closure and open-angle glaucoma: a comparison using optical coherence tomography. *Jpn J Ophthalmol* 2011;55(1):28-34.
- 39 Tamm ER, Ethier CR. Biological aspects of axonal damage in glaucoma: a brief review. *Exp Eye Res* 2017;157:5-12.
- 40 Sener H, Evreklioglu C, Horozoglu F, Sener ABG. Optic nerve head vessel density using OCTA in patients with primary angle closure disease: a systematic review and network meta-analysis. *Photodiagnosis Photodyn Ther* 2023;41:103209.
- 41 Lin B, Zuo C, Gao X, Huang D, Lin M. Quantitative measurements of vessel density and blood flow areas primary angle closure diseases: a study of optical coherence tomography angiography. *J Clin Med* 2022;11(14):4040.
- 42 Liu K, Xu H, Jiang H, Wang H, Wang P, Xu Y, Li F, Xu B, Yao X, Zou J. Macular vessel density and foveal avascular zone parameters in patients after acute primary angle closure determined by OCT angiography. *Sci Rep* 2020;10:18717.
- 43 Kim SB, Lee EJ, Han JC, Kee C. Comparison of peripapillary vessel density between preperimetric and perimetric glaucoma evaluated by OCT-angiography. *PLoS One* 2017;12(8):e0184297.

- 44 Richter GM, Madi I, Chu Z, Burkemper B, Chang R, Zaman A, Sylvester B, Reznik A, Kashani A, Wang RK, Varma R. Structural and functional associations of macular microcirculation in the ganglion cell-inner plexiform layer in glaucoma using optical coherence tomography angiography. *J Glaucoma* 2018;27(3):281-290.
- 45 Mansoori T, Balakrishna N. Peripapillary vessel density and retinal nerve fiber layer thickness in patients with unilateral primary angle closure glaucoma with superior hemifield defect. *J Curr Glaucoma Pract* 2019;13(1):21-27.
- 46 Wu J, Sebastian RT, Chu CJ, McGregor F, Dick AD, Liu L. Reduced macular vessel density and capillary perfusion in glaucoma detected using OCT angiography. *Curr Eye Res* 2019;44(5):533-540.
- 47 Holló G. Intrasession and between-visit variability of sector peripapillary angioflow vessel density values measured with the angiovue optical coherence tomograph in different retinal layers in ocular hypertension and glaucoma. *PLoS One* 2016;11(8):e0161631.